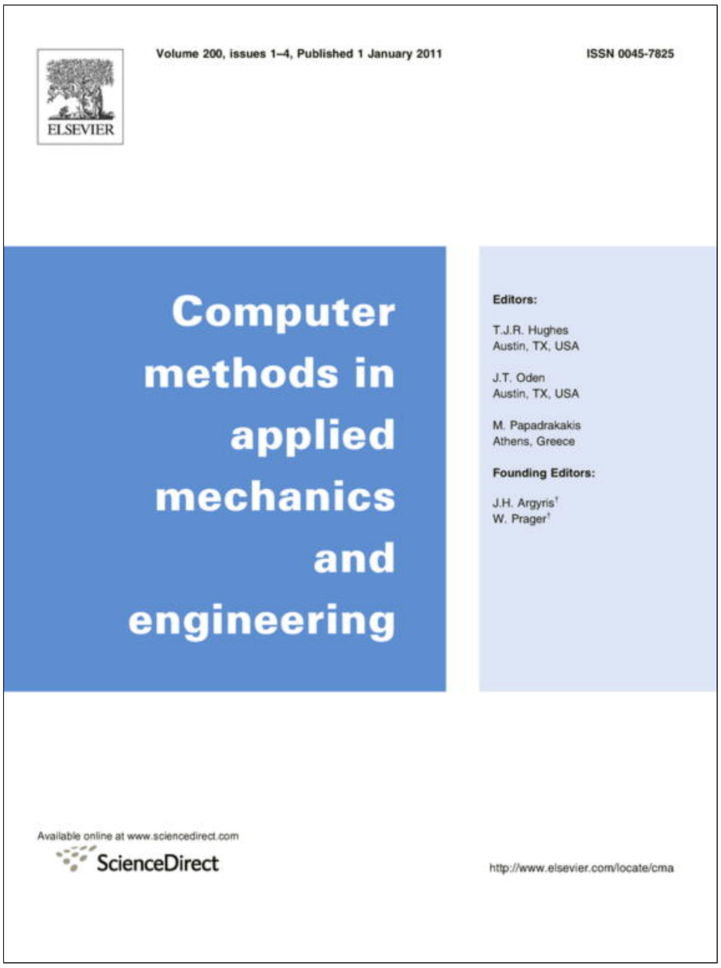
Volume 200, issues 1–4, Published 1 January 2011
ISSN 0045-7825
ELSEVIER
Computer methods in applied mechanics and engineering
Editors:
T.J.R. Hughes
Austin, TX, USA
J.T. Oden
Austin, TX, USA
M. Papadrakakis
Athens, Greece
Founding Editors:
J.H. Argyris†
W. Prager†
Available online at www.sciencedirect.com
ScienceDirect
http://www.elsevier.com/locate/cma

Comput. Methods Appl. Mech. Engrg. 200 (2011) 2498–2506

Contents lists available at ScienceDirect

Comput. Methods Appl. Mech. Engrg.

journal homepage: www.elsevier.com/locate/cma

Optimal control for quasi-Newtonian flows with defective boundary conditions

Hyesuk Lee

Department of Mathematical Sciences, Clemson University, Clemson, SC 29634-0975, USA

ARTICLE INFO

Article history:
Received 10 November 2010
Accepted 14 April 2011
Available online 24 April 2011

Keywords:
Quasi-Newtonian flow
Defective boundary condition
Optimal control

ABSTRACT

We consider a generalized-Newtonian fluid with defective boundary conditions where only flow rates or mean pressures are prescribed on parts of boundary. The defect boundary condition problem is formulated as an optimal control problem in which a Neumann or Dirichlet boundary control is used for matching given flow rates or mean pressures. For the constrained optimization problem an optimality system is derived from which a solution of the problem is obtained. Computational algorithms are discussed and numerical results are also presented.

1. Introduction

Many flow problems in real applications are modeled in an unbounded domain. Blood flows in the vascular system is one of the important applicative fields relative to such a situation. In simulating blood flow in a portion of vessel, an artificial boundary is introduced for upstream and downstream sections and a Dirichlet or Neumann type boundary condition is imposed on the boundary. However, in practice, those boundary data are not usually available, and sometimes recirculation of flow can occur near or on a boundary section. For this reason, in numerical simulation of such flows, it is more realistic to implement measurable data on the boundary such as pressure and flow rates.

Studies on flow problems with defective boundary conditions have been reported in [8,9,15,19]. In [8] Formaggia et al. discussed a defective boundary condition problem for the time dependent Navier–Stokes equation, where flow rates are specified on inflow and outflow boundaries. They introduced a Lagrange multiplier approach to enforce flow constraints at the inflow and outflow portions of the boundary. In [15] Heywood et al. also investigated the defective boundary condition problem for the time-dependent Navier–Stokes equations. For the specified flow rate problem, they considered construction of suitable *flux-carrier* vector functions. We used the Lagrange multiplier method in [8] to study a quasi-Newtonian flow problem with flow rate constraints in Sobolev spaces [7]. We established existence and uniqueness of solution for the continuous and discrete variational problems, and presented an error analysis for the numerical approximation. We could also observe that the flow field with flow rates boundary conditions looks very similar to that with a standard boundary condition; specified parabolic velocity inflow profiles and a "do nothing" outflow boundary condition.

Another defective boundary condition applicable in flow simulation is the mean pressure condition. In this case the mean pressure is specified on the inflow and outflow boundaries. In [15] the *do-nothing* approach was used to derive a particular weak formulation of the Navier–Sotkes equation with the mean pressure boundary condition. Similarly to a flow rate problem, the weak formulation involves implicit Neumann type boundary condition and chooses one particular solution from the set of all physical solutions satisfying the differential equation system.

In [9] Formaggia et al. studied the Stokes equations and the Navier–Stokes equations with defective boundary conditions in the setting of optimal control problems, where flow rate matching or mean pressure matching on boundaries is considered. A constant normal stress on each inflow or outflow boundary was chosen as a control for the matching. In the constraint equations the control appears in a boundary integral, which is referred to a boundary control [11].

The study of optimal control problems for Newtonian fluids has been very active in the last few decades (see [11–13] and references therein). In solving an optimal control problem with constraints, we can apply a sensitivity-based optimization scheme [3,14] or an adjoint-based optimization scheme [11,16]. For the adjoint-based optimization approach, the Lagrange multiplier method is used to derive an optimality system consisting of the fluid equations and the adjoint equations, from which an optimal solution is obtained. The sensitivity-based method requires solving so called *sensitivity equations*, which are derived by taking the Fréchet derivative of the operator associated with fluid equations with respect to control variables.

Studies on optimization for quasi-Newtonian flow are found in [1,5]. Du et al. [5] analyzed the optimal control problem for the

E-mail address: hklee@clemson.edu

0045-7825/$ - see front matter © 2011 Elsevier B.V. All rights reserved.
doi:10.1016/j.cma.2011.04.019

Ladyzhenskaya model using the Lagrange multipliers technique in the setting of Hilbert spaces. A shape optimization for blood flow was numerically investigated using the modified Cross model in [1].

The goal of this paper is to investigate finite element approximation of non-Newtonian flows with defective boundary conditions based on optimal control techniques. We develop numerical schemes applicable in physical and engineering problems such as blood flow system and polymer processing. We also compare performance of Dirichlet and Neumann boundary controls in the optimization problems. The approaches presented here are easily extendable to other flow control problems such as velocity tracking and drag minimization problems governed by non-Newtonian fluids.

This paper is organized as follows. In the remainder of this section, we describe the model problem, introduce function spaces and state an existence result. In Section 2 a flow rate boundary problem is formulated as an control problem using a Neumann control, and an optimality system is derived. We consider finite element approximation of the optimality system and a computational algorithm in Section 3, and in Section 4, we show how a Dirichlet control is implemented in variational formulation and discuss a numerical algorithm for the Dirichlet control problem. In Section 5, mean pressure boundary conditions are considered and finally, numerical results are presented in Section 6.

Let Ω be a bounded domain in $\mathbb{R}^n$ for $n = 2,3$ with boundary $\partial\Omega$. Suppose the boundary consists of the wall boundary Γ, inflow and outflow boundaries S_i, $i = 1,2,\ldots,m$. As a model problem for quasi-Newtonian flows consider the three-field Power law model

$$\boldsymbol{\sigma} = \nu_0|\mathbf{D}(\mathbf{u})|^{r-2}\mathbf{D}(\mathbf{u}) \quad \text{in } \Omega, \tag{1.1}$$

$$-\nabla\cdot\boldsymbol{\sigma} + \nabla p = \mathbf{f} \quad \text{in } \Omega, \tag{1.2}$$

$$div\, \mathbf{u} = 0 \quad \text{in } \Omega, \tag{1.3}$$

$$\mathbf{u} = \mathbf{0} \quad \text{on} \quad \Gamma, \tag{1.4}$$

subject to the specified flow rates on

$$S_i : \int_{S_i} \mathbf{u}\cdot\mathbf{n}\, dS = Q_i \text{ for } i = 1,\ldots,m,$$

where $\Gamma = \partial\Omega\backslash\cup_{i=1,\ldots,m}S_i$ and $\sum_{i=1}^m Q_i = 0$ for the incompressibility condition. For problems of physical interest, $1 < r \leqslant 2$, e.g. for shear thinning fluids. We denote its conjugate by r', satisfying $r^{-1} + r'^{-1} = 1$. Note that $r' \geqslant 2$ for $1 < r \leqslant 2$.

The constitutive equation of the fluid (1.1) can be rewritten as the inverted form

$$\mathbf{D}(\mathbf{u}) = \nu_0^{1-r'}|\boldsymbol{\sigma}|^{r'-2}\boldsymbol{\sigma} := G(\boldsymbol{\sigma}) \tag{1.6}$$

and the inverse is continuous [7]. It follows from [4] that $G(\cdot)$ satisfies

$$(G(s) - G(t)) : (s - t) \geqslant c|s - t|^{r'}, \quad \forall\, s,t \in \mathbb{R}^{n\times n}, \tag{1.7}$$

$$|G(s) - G(t)| \leqslant M(|s| + |t|)^{r'-2}|s - t|, \quad \forall\, s,t \in \mathbb{R}^{n\times n}. \tag{1.8}$$

Properties (1.7) and (1.8) imply that $G(\cdot)$ is strongly monotone, and Lipschitz continuous for bounded arguments [4].

The numerical approximation of the shear thinning flows with the homogeneous boundary condition has been previously studied in several papers [2,6,10,17,18]. There, the existence of a solution, a priori and a posteriori error estimates for the steady state problem were discussed.

Used in the analysis below are the following function spaces and norms.

$$\boldsymbol{\Sigma} := \left(L^{r'}(\Omega)\right)^{n\times n} = \left\{\boldsymbol{\tau} = (\tau_{ij});\ \tau_{ij} = \tau_{ji};\ \tau_{ij} \in L^{r'}(\Omega);\ i,j = 1,\ldots,n\right\},$$

with norm $\|\boldsymbol{\tau}\|_{\boldsymbol{\Sigma}} := (\int_\Omega |\boldsymbol{\tau}|^{r'} d\Omega)^{1/r'}$.

$$\mathbf{X} := \{\mathbf{v} \in (W^{1,r}(\Omega))^n : \mathbf{v}|_\Gamma = \mathbf{0}\},$$

with $W^{k,p}(\Omega)$ denoting the usual Sobolev space notation. We take for the norm on $\mathbf{X}$, $\|\mathbf{v}\|_{\mathbf{X}} := (\int_\Omega |\mathbf{D}(\mathbf{v})|^r d\Omega)^{1/r}$.

$$P := L^{r'}(\Omega),$$

with norm $\|q\|_P := \left(\int_\Omega |q|^{r'} d\Omega\right)^{1/r'}$. We use $\mathbf{V}$ to denote the subspace of $\mathbf{X}$ defined by

$$\mathbf{V} := \left\{\mathbf{v} \in \mathbf{X} : \int_\Omega q\nabla\cdot\mathbf{v}\, d\Omega = 0,\ \forall\ q \in P\right\}.$$

We use : and · to denote the scalar quantities $\boldsymbol{\sigma} : \boldsymbol{\tau} := \sum_{i=1}^n\sum_{j=1}^n \sigma_{ij}\tau_{ij}$ and $\mathbf{u}\cdot\mathbf{v} = \sum_{i=1}^n u_i v_i$.

If the flow rate defective boundary conditions (1.5) is replaced by the well defined Neumann condition

$$(\boldsymbol{\sigma} - pI)\cdot\mathbf{n} = \mathbf{g}_i \text{ on } S_i, \quad i = 1,2,\ldots,m, \tag{1.9}$$

the variational formulation to the problem is given as: determine $(\boldsymbol{\sigma},\mathbf{u},p) \in \boldsymbol{\Sigma}\times\mathbf{X}\times P$ such that

$$\nu_0^{1-r'}(|\boldsymbol{\sigma}|^{r'-2}\boldsymbol{\sigma},\boldsymbol{\tau}) - (\mathbf{D}(\mathbf{u}),\boldsymbol{\tau}) = 0, \quad \forall\ \boldsymbol{\tau} \in \boldsymbol{\Sigma}, \tag{1.10}$$

$$(\boldsymbol{\sigma},\mathbf{D}(\mathbf{v})) - (p,\nabla\cdot\mathbf{v}) = (\mathbf{f},\mathbf{v}) + \sum_{i=1}^m(\mathbf{g}_i,\mathbf{v})_{S_i}, \quad \forall\ \mathbf{v} \in \mathbf{X}, \tag{1.11}$$

$$(q,\nabla\cdot\mathbf{u}) = 0, \quad \forall\ q \in P. \tag{1.12}$$

Note that the velocity, pressure and stress spaces satisfy the following inf–sup conditions:

$$\inf_{q\in P}\sup_{\mathbf{v}\in\mathbf{X}} \frac{(q,\nabla\cdot\mathbf{v})}{\|\mathbf{v}\|_{\mathbf{X}}\|q\|_P} \geqslant C_{\mathbf{X}P}, \tag{1.13}$$

$$\inf_{\mathbf{v}\in\mathbf{X}}\sup_{\boldsymbol{\tau}\in\boldsymbol{\Sigma}} \frac{(\boldsymbol{\tau},\mathbf{D}(\mathbf{v}))}{\|\boldsymbol{\tau}\|_{\boldsymbol{\Sigma}}\|\mathbf{v}\|_{\mathbf{X}}} \geqslant C_{\boldsymbol{\Sigma}\mathbf{X}}. \tag{1.14}$$

The existence of a unique solution of (1.10)–(1.12) is established based on the inf–sup conditions (1.13) and (1.14) and the monotonicity (1.7) [2]. The estimate

$$\|\boldsymbol{\sigma}\|_{\boldsymbol{\Sigma}} + \|\mathbf{u}\|_{\mathbf{X}} + \|p\|_P \leqslant C(\|\mathbf{f}\|_{\mathbf{X}'} + \|\mathbf{g}\|_{\mathbf{M}}) \tag{1.15}$$

can be also shown as in [2].

2. The optimal control problem

2.1. Formulation of the problem

The defective boundary condition problem (1.1)–(1.5) can be formulated as an optimal control problem for flow rate matching. Suppose we choose the normal component of total stress

$$\mathbf{g} := \mathbf{g}_i := (\boldsymbol{\sigma} - pI)\mathbf{n} \text{ on } S_i, \quad i = 1,2,\ldots,m \tag{2.16}$$

as a control and let $S := \cup_{i=1}^m S_i$. Due to the condition $\sum_{i=1}^m Q_i = 0$ (or, equivalently $Q_1 = -\sum_{i=2}^m Q_i$), we set $\mathbf{g}_1 = (\boldsymbol{\sigma} - pI)\cdot\mathbf{n} = \mathbf{0}$ on S_1. For the control space, define $\mathbf{M} := (L^{r'}(S))^n$. The control affects the flow system through boundary integrals as shown in (1.11).

For the flow rate conditions (1.5), consider minimizing the penalized functional

$$\mathcal{J}(\mathbf{u},p,\boldsymbol{\sigma},\mathbf{g}) := \frac{1}{2}\sum_{i=1}^m\left(\int_{S_i}\mathbf{u}\cdot\mathbf{n}\, dS_i - Q_i\right)^2 + \frac{\epsilon}{r'}\int_S |\mathbf{g}|^{r'}\, dS, \tag{2.17}$$

where $\mathbf{g}$ is the Neumann boundary control chosen and ϵ is a penalty parameter. Then we formulate the optimal control problem in the following terms:

$$\text{Find}(\mathbf{u},p,\boldsymbol{\sigma},\mathbf{g}) \in \mathcal{U}_{ad} \text{ such that the functional(2.17)} \\ \text{is minimized subject to(1.10)–(1.12)}, \tag{2.18}$$

where the admissibility set $\mathcal{U}_{ad}$ is defined as follows.

$$\mathcal{U}_{ad} := \{(\mathbf{u},p,\boldsymbol{\sigma},\mathbf{g}) \in \mathbf{X}\times P\times \boldsymbol{\Sigma}\times \mathbf{M} : \mathcal{J}(\mathbf{u},p,\boldsymbol{\sigma},\mathbf{g}) < \infty\}. \tag{2.19}$$

The penalty term in (2.17) was introduced for several purposes. First, by the definition of the admissibility set (2.19), uniform boundedness of $\mathbf{g}$ is obtained immediately. Having the penalty term, we can implement various optimization schemes for computational algorithms, where the convergence rate is controllable by the penalty parameter ϵ. Also it was observed that the penalty term can be used to avoid the spurious local minimum by getting rid of unwanted oscillations [11].

2.2. Existence of an optimal control solution

The existence of an optimal solution of (2.18) is proven using standard arguments in the following theorem.

Theorem 2.1. *Given $\mathbf{f} \in \mathbf{X}'$, there exists a solution $(\mathbf{u},p,\sigma,\mathbf{g}) \in \mathbf{X}\times P\times\boldsymbol{\Sigma}\times\mathbf{M}$ of the optimal control problem (2.18).*

Proof. We first note that the admissible set $\mathcal{U}_{ad}$ is clearly not empty, e.g., $(\mathbf{u},p,\boldsymbol{\sigma},\mathbf{0}) \in \mathcal{U}_{ad}$. Let $\mathbf{g}_n$ be a minimizing sequence for the optimal control problem and set $\mathbf{u}_n = \mathbf{u}(\mathbf{g}_n)$, $p_n = p(\mathbf{g}_n)$, $\sigma_n = \sigma(\mathbf{g}_n)$. Then $(\mathbf{u}_n,p_n,\boldsymbol{\sigma}_n,\mathbf{g}_n) \in \mathcal{U}_{ad}$ for all n and satisfies

$$\lim_{n\to\infty} \mathcal{J}(\mathbf{u}_n,p_n,\boldsymbol{\sigma}_n,\mathbf{g}_n) = \inf_{(\mathbf{u},p,\boldsymbol{\sigma},\mathbf{g})\in\mathcal{U}_{ad}} \mathcal{J}(\mathbf{u},p,\boldsymbol{\sigma},\mathbf{g}).$$

By the definition of $\mathcal{U}_{ad}$, we have

$$v_0^{1-r'}(|\boldsymbol{\sigma}_n|^{r'-2}\boldsymbol{\sigma}_n,\boldsymbol{\tau}) - (\mathbf{D}(\mathbf{u}_n),\boldsymbol{\tau}) = 0, \quad \forall\, \boldsymbol{\tau} \in \boldsymbol{\Sigma}, \tag{2.20}$$

$$(\boldsymbol{\sigma}_n,\mathbf{D}(\mathbf{v})) - (p_n,\nabla\cdot\mathbf{v}) = (\mathbf{f},\mathbf{v}) + (\mathbf{g}_n,\mathbf{v})_S, \quad \forall\, \mathbf{v}\in\mathbf{X}, \tag{2.21}$$

$$(q,\nabla\cdot\mathbf{u}_n) = 0, \quad \forall\, q \in P. \tag{2.22}$$

The sequence $\mathbf{g}_n$ is uniformly bounded in $\mathbf{M}$ from (2.19) and the corresponding $(\mathbf{u}_n,p_n,\sigma_n)$ is uniformly bounded in $\mathbf{X}\times P\times\boldsymbol{\Sigma}$ from (1.15). We may then extract subsequences, still denoted by $(\mathbf{u}_n,p_n,\sigma_n,\mathbf{g}_n)$, such that

$$\begin{aligned} &\mathbf{g}_n \rightharpoonup \tilde{\mathbf{g}} \quad \text{in } \mathbf{M},\\ &p_n \rightharpoonup \tilde{p} \quad \text{in } P,\\ &\mathbf{u}_n \rightharpoonup \tilde{\mathbf{u}} \quad \text{in } \mathbf{X},\\ &\boldsymbol{\sigma}_n \rightharpoonup \tilde{\boldsymbol{\sigma}} \quad \text{in } \boldsymbol{\Sigma},\\ &\mathbf{u}_n \to \tilde{\mathbf{u}} \quad \text{in } (L^r(\Omega))^n \end{aligned}$$

for some $(\tilde{\mathbf{u}},\tilde{p},\tilde{\boldsymbol{\sigma}},\tilde{\mathbf{g}}) \in \mathbf{X}\times P\times\boldsymbol{\Sigma}\times\mathbf{M}$. The last convergence result above follows from the compact embedding of $(W^{1,r}(\Omega))^n$. We may pass to the limit in (1.10)–(1.12) to determine that $(\tilde{\mathbf{u}},\tilde{p},\tilde{\boldsymbol{\sigma}},\tilde{\mathbf{g}})$ satisfies (1.10)–(1.12). The only trouble term when one passes to the limit is the nonlinearity $(|\boldsymbol{\sigma}_n|^{r'-2}\boldsymbol{\sigma}_n,\boldsymbol{\tau})$. However, since $G(\cdot)$ is a monotone operator, G is sequential weak continuous [20], and therefore,

$$\lim_{n\to\infty}(|\boldsymbol{\sigma}_n|^{r'-2}\boldsymbol{\sigma}_n,\boldsymbol{\tau}) = (|\tilde{\boldsymbol{\sigma}}|^{r'-2}\tilde{\boldsymbol{\sigma}},\boldsymbol{\tau}), \quad \forall\, \boldsymbol{\tau}\in\boldsymbol{\Sigma}.$$

We have shown that $(\tilde{\mathbf{u}},\tilde{p},\tilde{\boldsymbol{\sigma}},\tilde{\mathbf{g}})$ indeed satisfies (1.10)–(1.12). Now, by the weak lower semi-continuity of $\mathcal{J}(\cdot,\cdot,\cdot,\cdot)$, we conclude that $(\tilde{\mathbf{u}},\tilde{p},\tilde{\boldsymbol{\sigma}},\tilde{\mathbf{g}})$ is an optimal solution i.e.,

$$\inf_{(\mathbf{u},p,\boldsymbol{\sigma},\mathbf{g})\in\mathcal{U}_{ad}} \mathcal{J}(\mathbf{u},p,\boldsymbol{\sigma},\mathbf{g}) = \lim_{n\to\infty}\mathcal{J}(\mathbf{u}_n,p_n,\boldsymbol{\sigma}_n,\mathbf{g}_n) = \mathcal{J}(\tilde{\mathbf{u}},\tilde{p},\tilde{\boldsymbol{\sigma}},\tilde{\mathbf{g}}).$$

Thus, we have shown that an optimal solution belonging to $\mathcal{U}_{ad}$ exists. □

2.3. Adjoint system

A constrained optimal control problem is often solved by the adjoint-based method using the Lagrange multiplier's rule [11]. In this paper we use the method without considering analysis related to Lagrange multipliers such as existence and regularity of adjoint variables.

For $(\mathbf{u},\boldsymbol{\sigma},p,\mathbf{g})$, define the Lagrangian

$$\begin{aligned}\mathcal{L}(\mathbf{u},\boldsymbol{\sigma},p,\mathbf{g},\mathbf{w},\boldsymbol{\eta},\xi) &= \mathcal{J}(\mathbf{u},p,\boldsymbol{\sigma},\mathbf{g}) + v_0^{1-r'}(|\boldsymbol{\sigma}|^{r'-2}\boldsymbol{\sigma},\boldsymbol{\eta})\\ &\quad - (\mathbf{D}(\mathbf{u}),\boldsymbol{\eta}) + (\boldsymbol{\sigma},\mathbf{D}(\mathbf{w})) - (p,\nabla\cdot\mathbf{w})\\ &\quad - \langle\mathbf{f},\mathbf{w}\rangle - (\mathbf{g},\mathbf{w})_S - (\xi,\nabla\cdot\mathbf{u}).\end{aligned} \tag{2.23}$$

Using the first order necessary conditions, $\frac{\partial\mathcal{L}}{\partial\boldsymbol{\sigma}} = 0$, $\frac{\partial\mathcal{L}}{\partial\mathbf{u}} = 0$ and $\frac{\partial\mathcal{L}}{\partial p} = 0$, the adjoint system is derived as

$$v_0^{1-r'}(r'-2)(|\boldsymbol{\sigma}|^{r'-4}(\boldsymbol{\sigma}:\boldsymbol{\eta})\boldsymbol{\sigma},\boldsymbol{\tau}) + v_0^{1-r'}(|\boldsymbol{\sigma}|^{r'-2}\boldsymbol{\eta},\boldsymbol{\tau}) + (\mathbf{D}(\mathbf{w}),\boldsymbol{\tau}) = 0, \quad \forall\,\boldsymbol{\tau}\in\boldsymbol{\Sigma}, \tag{2.24}$$

$$(\boldsymbol{\eta},\mathbf{D}(\mathbf{v})) + (\xi,\nabla\cdot\mathbf{v}) = \sum_{i=1}^m\left(\int_{S_i}\mathbf{u}\cdot\mathbf{n}\,dS_i - Q_i\right)\times\int_{S_i}\mathbf{v}\cdot\mathbf{n}\,dS_i, \quad \forall\,\mathbf{v}\in\mathbf{X}, \tag{2.25}$$

$$(q,\nabla\cdot\mathbf{w}) = 0, \quad \forall\, q\in P, \tag{2.26}$$

where $\mathbf{w}$, ξ, $\boldsymbol{\eta}$ are the adjoint velocity, pressure and stress, respectively. Also using $\frac{\partial\mathcal{L}}{\partial\mathbf{g}} = 0$, we obtain the optimality condition

$$\int_S |\mathbf{g}|^{r'-2}\mathbf{g}\cdot\mathbf{h}\,dS = \frac{1}{\epsilon}\int_S \mathbf{w}\cdot\mathbf{h}\,dS, \quad \forall\,\mathbf{h}\in\mathbf{M}, \tag{2.27}$$

which yields an explicit formula for the control $\mathbf{g}$ in terms of the adjoint variable $\mathbf{w}$ as

$$\mathbf{g} = \frac{1}{\epsilon^{r/r'}}|\mathbf{w}|^{r-2}\mathbf{w} \quad \text{on } S. \tag{2.28}$$

Therefore, the state governing Eqs. (1.10)–(1.12), the optimality condition (2.28) and the adjoint Eqs. (2.24)–(2.26) form a coupled optimality system:

$$v_0^{1-r'}(|\boldsymbol{\sigma}|^{r'-2}\boldsymbol{\sigma},\boldsymbol{\tau}) - (\mathbf{D}(\mathbf{u}),\boldsymbol{\tau}) = 0, \quad \forall\,\boldsymbol{\tau}\in\boldsymbol{\Sigma}, \tag{2.29}$$

$$(\boldsymbol{\sigma},\mathbf{D}(\mathbf{v})) - (p,\nabla\cdot\mathbf{v}) = (\mathbf{f},\mathbf{v}) + \frac{1}{\epsilon^{r/r'}}(|\mathbf{w}|^{r-2}\mathbf{w},\mathbf{v})_S, \quad \forall\,\mathbf{v}\in\mathbf{X}, \tag{2.30}$$

$$(q,\nabla\cdot\mathbf{u}) = 0, \quad \forall\, q\in P, \tag{2.31}$$

$$v_0^{1-r'}(r'-2)(|\boldsymbol{\sigma}|^{r'-4}(\boldsymbol{\sigma}:\boldsymbol{\eta})\boldsymbol{\sigma},\boldsymbol{\tau}) + v_0^{1-r'}(|\boldsymbol{\sigma}|^{r'-2}\boldsymbol{\eta},\boldsymbol{\tau}) + (\mathbf{D}(\mathbf{w}),\boldsymbol{\tau}) = 0, \quad \forall\,\boldsymbol{\tau}\in\boldsymbol{\Sigma}, \tag{2.32}$$

$$(\boldsymbol{\eta},\mathbf{D}(\mathbf{v})) + (\xi,\nabla\cdot\mathbf{v}) = \sum_{i=1}^m\left(\int_{S_i}\mathbf{u}\cdot\mathbf{n}\,dS_i - Q_i\right)\times\int_{S_i}\mathbf{v}\cdot\mathbf{n}\,dS_i, \quad \forall\,\mathbf{v}\in\mathbf{X}, \tag{2.33}$$

$$(q,\nabla\cdot\mathbf{w}) = 0, \quad \forall\, q\in P. \tag{2.34}$$

Remark 2.2. The adjoint problem (2.32) is defined in a correct function space. Note that

$$\int_\Omega |\boldsymbol{\sigma}|^{rr'-4r}(\boldsymbol{\sigma}:\boldsymbol{\eta})^r|\boldsymbol{\sigma}|^r\,d\Omega \leqslant \int_\Omega |\boldsymbol{\sigma}|^{rr'-4r}|\boldsymbol{\eta}|^r|\boldsymbol{\sigma}|^{2r}\,d\Omega = \int_\Omega |\boldsymbol{\sigma}|^{r'-r}|\boldsymbol{\eta}|^r\,d\Omega \tag{2.35}$$

and using the Hölder's inequality,

$$\int_\Omega |\boldsymbol{\sigma}|^{r'-r}|\boldsymbol{\eta}|^r \, d\Omega \leqslant \left(\int_\Omega (|\boldsymbol{\sigma}|^{r'-r})^p \, d\Omega\right)^{1/p} \left(\int_\Omega (|\boldsymbol{\eta}|^r)^q \, d\Omega\right)^{1/q},$$

$$\text{where } p = \frac{r'}{r'-r} \text{ and } q = \frac{r'}{r} = \|\boldsymbol{\sigma}\|_\Sigma^{r'-r}\|\boldsymbol{\eta}\|_\Sigma^r < \infty. \tag{2.36}$$

Therefore, $|\boldsymbol{\sigma}|^{r'-4}(\boldsymbol{\sigma}:\boldsymbol{\eta})\boldsymbol{\sigma}, |\boldsymbol{\sigma}|^{r'-2}\boldsymbol{\eta} \in (L^r(\Omega))^{n\times n}$ for $\eta \in \boldsymbol{\Sigma}$.

For the adjoint system above, define the linear operator $\bar{A}$ defined on $\boldsymbol{\Sigma}\times\boldsymbol{\Sigma}$ by

$$\bar{A}(\boldsymbol{\eta},\boldsymbol{\tau}) := v_0^{1-r'}(r'-2)(|\boldsymbol{\sigma}|^{r'-4}(\boldsymbol{\sigma}:\boldsymbol{\eta})\boldsymbol{\sigma},\boldsymbol{\tau}) + v_0^{1-r'}(|\boldsymbol{\sigma}|^{r'-2}\boldsymbol{\eta},\boldsymbol{\tau}). \tag{2.37}$$

Using the adjoint bilinear form $\bar{A}$ defined by (2.37), the adjoint equations in (2.24)–(2.26) can be equivalently written as

$$\bar{A}(\boldsymbol{\eta},\boldsymbol{\tau}) + (\mathbf{D}(\mathbf{w}),\boldsymbol{\tau}) = \mathbf{0}, \quad \forall\, \boldsymbol{\tau}\in\boldsymbol{\Sigma}, \tag{2.38}$$

$$(\boldsymbol{\eta}, D(\mathbf{v})) = \sum_{i=1}^m \left(\int_{S_i} \mathbf{u}\cdot\mathbf{n}dS - Q_i\right)\int_{S_i}\mathbf{v}\cdot\mathbf{n}dS_i, \quad \forall\, \mathbf{v}\in\mathbf{V}. \tag{2.39}$$

Lemma 2.3. *The adjoint operator $\bar{A}$ is Lipschitz continuous and strictly monotone.*

Proof. First, we show the continuity:

$$\begin{aligned}
&v_0^{1-r'}(r'-2)(|\boldsymbol{\sigma}|^{r'-4}(\boldsymbol{\sigma}:\boldsymbol{\eta})\boldsymbol{\sigma},\boldsymbol{\tau}) + v_0^{1-r'}(|\boldsymbol{\sigma}|^{r'-2}\boldsymbol{\eta},\boldsymbol{\tau})\\
&\leqslant C\left(\||\boldsymbol{\sigma}|^{r'-4}(\boldsymbol{\sigma}:\boldsymbol{\eta})\boldsymbol{\sigma}\|_{L^{r}(\Omega)}\|\boldsymbol{\tau}\|_\Sigma + \||\boldsymbol{\sigma}|^{r'-2}\boldsymbol{\eta}\|_{L^{r}(\Omega)}\|\boldsymbol{\tau}\|_\Sigma\right)\\
&\leqslant C\left[\left(\int_\Omega |\boldsymbol{\sigma}|^{rr'-4r}(\boldsymbol{\sigma}:\boldsymbol{\eta})^r|\boldsymbol{\sigma}|^r\, d\Omega\right)^{1/r} + \left(\int_\Omega |\boldsymbol{\sigma}|^{rr'-2r}|\boldsymbol{\eta}|^r\, d\Omega\right)^{1/r}\right]\|\boldsymbol{\tau}\|_\Sigma\\
&\leqslant C\left(\int_\Omega |\boldsymbol{\sigma}|^{r'-r}|\boldsymbol{\eta}|^r\, d\Omega\right)^{1/r}\|\boldsymbol{\tau}\|_\Sigma\\
&\leqslant C\left(\|\boldsymbol{\sigma}\|_\Sigma^{r'-r}\|\boldsymbol{\eta}\|_\Sigma^r\right)^{1/r}\|\boldsymbol{\tau}\|_\Sigma \text{ using (2.36)}\\
&\leqslant C\|\boldsymbol{\sigma}\|_\Sigma^{r'-2}\|\boldsymbol{\eta}\|_\Sigma\|\boldsymbol{\tau}\|_\Sigma \leqslant C\|\boldsymbol{\eta}\|_\Sigma\|\boldsymbol{\tau}\|_\Sigma \text{ by (1.15) and (2.19).}
\end{aligned} \tag{2.40}$$

Strict monotonicity can be easily seen as

$$\bar{A}(\boldsymbol{\eta},\boldsymbol{\eta}) = v_0^{1-r'}(r'-2)\int_\Omega |\boldsymbol{\sigma}|^{r'-4}(\boldsymbol{\sigma}:\boldsymbol{\eta})^2\, d\Omega + v_0^{1-r'}\int_\Omega |\boldsymbol{\sigma}|^{r'-2}|\boldsymbol{\eta}|^2\, d\Omega > 0$$

for $\eta \neq \mathbf{0}$. □

Remark 2.4. Unfortunately, the solvability of the adjoint problem (2.38) and (2.39) is not clear as coercivity of the operator $\bar{A}$ can not be shown. However, when discretized, one can show the existence of a finite element approximate solution. See Theorem 3.1.

3. Finite element approximation

3.1. Finite element spaces

Suppose T_h is a triangulation of Ω such that $\bar{\Omega} = \{\bigcup K : K\in T_h\}$. Assume that there exist positive constants c_1, c_2 such that

$c_1\rho_K \leqslant h_K \leqslant c_2\rho_K$,

where h_K is the diameter of K, ρ_K is the diameter of the greatest ball included in K, and $h = \max_{K\in T_h} h_K$.

Let $P_k(K)$ denote the space of polynomials of degree less than or equal to k on $K\in T_h$. We define finite element spaces for an approximation of $(\mathbf{u},p,\boldsymbol{\sigma})$:

$$\begin{aligned}
\mathbf{X}^h &:= \{\mathbf{v}\in\mathbf{X}\cap(C^0(\bar{\Omega}))^n : \mathbf{v}|_K\in P_k(K),\ \forall\, K\in T_h\},\\
P^h &:= \{q\in P\cap(C^0(\bar{\Omega})) : q|_K\in P_m(K),\ \forall\, K\in T_h\},\\
\boldsymbol{\Sigma}^h &:= \{\boldsymbol{\tau}\in\boldsymbol{\Sigma}\cap(C^0(\bar{\Omega}))^{n\times n} : \boldsymbol{\tau}|_K\in P_l(K),\ \forall K\ \in T_h\},\\
\mathbf{V}^h &:= \{\mathbf{v}\in\mathbf{X}^h : (q,\nabla\cdot\mathbf{v}) = 0,\ \forall\, q\in P^h\}.
\end{aligned}$$

We assume that the velocity-stress and the pressure–velocity space satisfy the following discrete inf–sup (or LBB) conditions [2]: There exist constants $C_{XPh}, C_{\Sigma Xh} > 0$ such that

$$\inf_{0\neq q^h\in P^h}\sup_{0\neq\mathbf{v}^h\in\mathbf{X}^h}\frac{(q^h,\nabla\cdot\mathbf{v}^h)}{\|\mathbf{v}^h\|_\mathbf{X}\|q^h\|_P} \geqslant C_{XPh}, \tag{3.1}$$

$$\inf_{0\neq\mathbf{v}^h\in\mathbf{X}^h}\sup_{0\neq\boldsymbol{\tau}^h\in\boldsymbol{\Sigma}^h}\frac{(\boldsymbol{\tau}^h,\mathbf{D}(\mathbf{v}^h))}{\|\boldsymbol{\tau}^h\|_\Sigma\|\mathbf{v}^h\|_\mathbf{X}} \geqslant C_{\Sigma Xh}. \tag{3.2}$$

The finite element approximation of (1.10)–(1.12) is then as follows: find $\mathbf{u}^h\in\mathbf{X}^h$, $p^h\in P^h$, $\boldsymbol{\sigma}^h\in\boldsymbol{\Sigma}^h$ such that

$$v_0^{1-r'}(|\boldsymbol{\sigma}^h|^{r'-2}\boldsymbol{\sigma}^h,\boldsymbol{\tau}^h) - (\mathbf{D}(\mathbf{u}^h),\boldsymbol{\tau}^h) = 0, \quad \forall\,\boldsymbol{\tau}^h\in\boldsymbol{\Sigma}^h, \tag{3.3}$$

$$(\boldsymbol{\sigma}^h,\mathbf{D}(\mathbf{v}^h)) - (p^h,\nabla\cdot\mathbf{v}^h) = (\mathbf{f},\mathbf{v}^h) + \frac{1}{\epsilon^{r/r'}}(|\mathbf{w}^h|^{r-2}\mathbf{w}^h,\mathbf{v}^h)_S, \quad \forall\,\mathbf{v}^h\in\mathbf{X}^h, \tag{3.4}$$

$$(q^h,\nabla\cdot\mathbf{u}^h) = 0, \quad \forall\, q^h\in P^h. \tag{3.5}$$

Existence result and error estimates for the finite element solution of (3.3)–(3.5) can be found in [2,7] for a given $\mathbf{w}^h$.

Finite element approximation of the adjoint system reads as:

$$v_0^{1-r'}(r'-2)(|\boldsymbol{\sigma}^h|^{r'-4}(\boldsymbol{\sigma}^h:\boldsymbol{\eta}^h)\boldsymbol{\sigma}^h,\boldsymbol{\tau}^h) + v_0^{1-r'}(|\boldsymbol{\sigma}^h|^{r'-2}\boldsymbol{\eta}^h,\boldsymbol{\tau}^h) + (\mathbf{D}(\mathbf{w}^h),\boldsymbol{\tau}^h) = 0, \quad \forall\,\boldsymbol{\tau}^h\in\boldsymbol{\Sigma}^h, \tag{3.6}$$

$$(\boldsymbol{\eta}^h,\mathbf{D}(\mathbf{v}^h)) + (\xi^h,\nabla\cdot\mathbf{v}^h) = \sum_{i=1}^m\left(\int_{S_i}\mathbf{u}^h\cdot\mathbf{n}\, dS_i - Q_i\right)\times\int_{S_i}\mathbf{v}^h\cdot\mathbf{n}\, dS_i, \quad \forall\,\mathbf{v}^h\in\mathbf{X}^h, \tag{3.7}$$

$$(q^h,\nabla\cdot\mathbf{w}^h) = 0, \quad \forall\, q^h\in P^h, \tag{3.8}$$

Theorem 3.1. *For given $\mathbf{u}^h\in\mathbf{X}^h$ and $\sigma^h\in\boldsymbol{\Sigma}^h$, the discrete linear adjoint system (3.6)–(3.8) admits a unique solution $(\mathbf{w}^h,\xi^h,\eta^h)\in\mathbf{X}^h\times P^h\times\boldsymbol{\Sigma}^h$.*

Proof. In the discrete div free space $\mathbf{V}^h$, the adjoint problem is equivalent to

$$\bar{A}^h(\boldsymbol{\eta}^h,\boldsymbol{\tau}^h) + (D(\mathbf{w}^h),\boldsymbol{\tau}^h) = \mathbf{0}, \quad \forall\,(\mathbf{v}^h,\boldsymbol{\tau}^h)\in\mathbf{V}^h\times\boldsymbol{\Sigma}^h, \tag{3.9}$$

$$(\boldsymbol{\eta}^h,D(\mathbf{v}^h)) = \sum_{i=1}^m\left(\int_{S_i}\mathbf{u}^h\cdot\mathbf{n}\, dS_i - Q_i\right)\int_{S_i}\mathbf{v}^h\cdot\mathbf{n}, \quad \forall\,\mathbf{v}^h\in\mathbf{V}^h, \tag{3.10}$$

where $\bar{A}^h$ is a discrete adjoint operator defined analogously to (2.37). Note that the system (3.9) and (3.10) is a saddle point problem defined in the div free space $\mathbf{V}^h$.

The operator $\bar{A}^h$ is symmetric and positive definite by Lemma 2.3. Therefore, by the inf–sup condition (3.2) there exists of a unique $(\mathbf{w}^h,\eta^h)$ satisfying (3.9) and (3.10). The existence and uniqueness of ξ^h then follows from the inf–sup condition (3.1). □

3.2. Computational algorithm

The optimality system is a coupled system whose solution yields a solution of the optimization problem (2.18). In practice, the size of the system is huge, and therefore, the state and adjoint systems need to be decoupled. One way of accomplishing this is through a gradient type method. The gradient method for minimizing the functional $\mathcal{M}(\mathbf{g}) := \mathcal{J}(\mathbf{u}(\mathbf{g}),p(\mathbf{g}),\boldsymbol{\sigma}(\mathbf{g}),\mathbf{g})$ is given as the form

$$\mathbf{g}_{(k+1)} = \mathbf{g}_{(k)} - \rho_k \frac{d\mathcal{M}}{d\mathbf{g}_k}, \tag{3.11}$$

where ρ_k is a step size. The gradient of the function $\frac{d\mathcal{M}}{d\mathbf{g}_k}$ can be determined by a solution of the adjoint system by the optimality condition (2.28) [11]:

$$\frac{d\mathcal{M}}{d\mathbf{g}_k} = \epsilon|\mathbf{g}_k|^{r'-2}\mathbf{g}_k - \mathbf{w}_k|_S. \tag{3.12}$$

Choosing the step size dependent on the penalty parameter ϵ, i.e., $\rho_k = \alpha_k/\epsilon$ and using (3.12), the steepest decent algorithm for $\mathbf{g}_k$ is written as

$$\mathbf{g}_{k+1} = (1 - \alpha_k|\mathbf{g}_k|^{r'-2})\mathbf{g}_k + \frac{\alpha_k}{\epsilon}\mathbf{w}_k|_S. \tag{3.13}$$

Since the size of coupled optimality system is large and the gradient of the functional (3.12) involves only the control and an adjoint variable, the steepest decent type method can be used as an minimizing routine while also decoupling the system. The computational algorithm is then given as follows.

Algorithm 3.2. (Steepest descent algorithm)

Choose the initial control $\mathbf{g}_0^h$.
For $k = 0, 1, \ldots$

1. Solve (3.3), (3.5) and
$$(\boldsymbol{\sigma}^h, \mathbf{D}(\mathbf{v}^h)) - (p^h, \nabla\cdot\mathbf{v}^h) = (\mathbf{f}, \mathbf{v}^h) + (\mathbf{g}_k^h, \mathbf{v}^h)_S$$
for $(\mathbf{u}_k^h, p_k^h, \boldsymbol{\sigma}_k^h)$.
2. Solve (3.6)–(3.8) for $\left(\mathbf{w}_k^h, \xi_k^h, \boldsymbol{\eta}_k^h\right)$.
3. Update the control by (3.13).

Here the step size α_k can be chosen optimally in each iteration or a constant step size ρ may be used in all iterations. The convergence property of the above algorithm can be obtained in the standard manner. Other methods such as the trust region method and a Newton-type method may be considered as a minimization algorithm.

4. Dirichlet control

In this section we consider a Dirichlet boundary control for the flow rate condition. Choosing

$$\mathbf{g} := \mathbf{g}_i := \mathbf{u} \quad \text{on } S_i, \quad i = 1, 2, \ldots, m \tag{4.14}$$

as a control satisfying

$$\int_S \mathbf{g}\cdot\mathbf{n}\, dS = 0 \tag{4.15}$$

for the incompressibility condition, imposing the Dirichlet boundary condition weakly and combining with the mass conservation equation in a variation formulation, we obtain the following form:

$$\nu_0^{1-r'}(|\boldsymbol{\sigma}|^{r'-2}\boldsymbol{\sigma}, \boldsymbol{\tau}) - (\mathbf{D}(\mathbf{u}), \boldsymbol{\tau}) = 0, \quad \forall \boldsymbol{\tau} \in \boldsymbol{\Sigma}, \tag{4.16}$$

$$(\boldsymbol{\sigma}, \mathbf{D}(\mathbf{v})) - (p, \nabla\cdot\mathbf{v}) - (\mathbf{t}, \mathbf{v})_S = (\mathbf{f}, \mathbf{v}), \quad \forall \mathbf{v} \in \mathbf{X}, \tag{4.17}$$

$$(q, \nabla\cdot\mathbf{u}) + (\mathbf{z}, \mathbf{u})_S = (\mathbf{g}, \mathbf{z})_S, \quad \forall (q, \mathbf{z}) \in P \times (W^{1/r-1,r}(S))^n. \tag{4.18}$$

In (4.17) the additional unknown function $\mathbf{t} \in (W^{1/r-1,r}(S))^n$ represents the stress force on S and $\mathbf{g}$ belongs to the control space defined as $M := \left\{\mathbf{h} \in (W^{1,r}(S))^n : \int_S \mathbf{h}\cdot\mathbf{n}\, dS = 0\right\}$.

Remark 4.1. The system (4.16)–(4.18) is formulated as a twofold saddle point problem as in (1.10)–(1.12), of the form

$$\nu_0^{1-r'}(|\boldsymbol{\sigma}|^{r'-2}\boldsymbol{\sigma}, \boldsymbol{\tau}) - (\mathbf{D}(\mathbf{u}), \boldsymbol{\tau}) = 0, \tag{4.19}$$

$$(\boldsymbol{\sigma}, \mathbf{D}(\mathbf{v})) - \gamma((p, \mathbf{t}), \mathbf{v}) = (\mathbf{f}, \mathbf{v}), \tag{4.20}$$

$$\gamma((q, \mathbf{z}), \mathbf{u}) = (\mathbf{g}, \mathbf{z})_S, \tag{4.21}$$

where $\gamma((p, \mathbf{t}), \mathbf{v}) := (p, \nabla\cdot\mathbf{v}) + (\mathbf{t}, \mathbf{v})_S$. Therefore, the bilinear form $\gamma((\cdot,\cdot),\cdot)$ needs to satisfy the inf–sup condition for the existence and uniqueness of a solution. Such analytical issues will be addressed in a later paper.

For the Dirichlet control we consider the functional

$$\mathcal{J}(\mathbf{u}, p, \boldsymbol{\sigma}, \mathbf{g}) := \frac{1}{2}\sum_{i=1}^{m}\left(\int_{S_i}\mathbf{u}\cdot\mathbf{n}\, dS_i - Q_i\right)^2 + \frac{\epsilon}{r}\int_S |\nabla_s\mathbf{g}|^r + |\mathbf{g}|^r\, dS, \tag{4.22}$$

where ∇_s denotes the surface gradient. It is known that the gradient term in the penalty integral in (4.22) provides more regularity of the control and reduces oscillatory behavior of iterations near a minimizer [11]. We define the Lagrangian

$$\begin{aligned}\mathcal{L}(\mathbf{u}, \boldsymbol{\sigma}, p, \mathbf{t}, \mathbf{g}, \mathbf{w}, \boldsymbol{\eta}, \xi, \mathbf{s}) = {}& \mathcal{J}(\mathbf{u}, p, \boldsymbol{\sigma}, \mathbf{g}) + \nu_0^{1-r'}(|\boldsymbol{\sigma}|^{r'-2}\boldsymbol{\sigma}, \boldsymbol{\eta}) \\ & - (\mathbf{D}(\mathbf{u}), \boldsymbol{\eta}) + (\boldsymbol{\sigma}, \mathbf{D}(\mathbf{w})) - (p, \nabla\cdot\mathbf{w}) \\ & - (\mathbf{t}, \mathbf{w})_S - \langle \mathbf{f}, \mathbf{w}\rangle - (\xi, \nabla\cdot\mathbf{u}) \\ & - (\mathbf{u}, \mathbf{s})_S + (\mathbf{g}, \mathbf{s})_S + \lambda(\mathbf{g}, \mathbf{n})_S,\end{aligned} \tag{4.23}$$

where the last term in (4.23) was added to enforce the condition (4.15). Using the same arguments in Section 2, the adjoint system is derived as

$$\nu_0^{1-r'}(r'-2)(|\boldsymbol{\sigma}|^{r'-4}(\boldsymbol{\sigma}:\boldsymbol{\eta})\boldsymbol{\sigma}, \boldsymbol{\tau}) + \nu_0^{1-r'}(|\boldsymbol{\sigma}|^{r'-2}\boldsymbol{\eta}, \boldsymbol{\tau}) + (\mathbf{D}(\mathbf{w}), \boldsymbol{\tau}) = 0, \quad \forall\, \boldsymbol{\tau} \in \boldsymbol{\Sigma}, \tag{4.24}$$

$$(\boldsymbol{\eta}, \mathbf{D}(\mathbf{v})) + (\xi, \nabla\cdot\mathbf{v}) + (\mathbf{s}, \mathbf{v})_S = \sum_{i=1}^{m}\left(\int_{S_i}\mathbf{u}\cdot\mathbf{n}\, dS_i - Q_i\right) \times \int_{S_i}\mathbf{v}\cdot\mathbf{n}\, dS_i, \quad \forall\, \mathbf{v} \in \mathbf{X}, \tag{4.25}$$

$$-(q, \nabla\cdot\mathbf{w}) - (\mathbf{z}, \mathbf{w})_S = 0, \quad \forall\, (q, \mathbf{z}) \in P \times (W^{1/r-1,r}(S))^n, \tag{4.26}$$

where $\mathbf{w}$, ξ, $\boldsymbol{\eta}$, $\mathbf{s}$ are the adjoint velocity, pressure, stress and stress force, respectively. Also by $\frac{\partial\mathcal{L}}{\partial\mathbf{g}} = 0$, we obtain the optimality condition

$$\int_S \epsilon|\nabla_s\mathbf{g}|^{r-2}\nabla_s\mathbf{g}\cdot\nabla_s\mathbf{h} + \epsilon|\mathbf{g}|^{r-2}\mathbf{g}\cdot\mathbf{h} + \mathbf{s}\cdot\mathbf{h} + \lambda\mathbf{n}\cdot\mathbf{h}\, dS = 0, \quad \forall\, \mathbf{h} \in M. \tag{4.27}$$

Note that this condition yields a differential equation to be solved for the control on S. Implementing the steepest decent algorithm to update the control, we have the following variational form: find $(\mathbf{g}_{k+1}, \lambda_{k+1}) \in (W^{1,r}(S))^n \times \mathbb{R}$ satisfying

$$\begin{aligned}&(|\nabla_s\mathbf{g}_{k+1}|^{r-2}\nabla_s\mathbf{g}_{k+1}, \nabla_s\mathbf{h})_S + (|\mathbf{g}_{k+1}|^{r-2}\mathbf{g}_{k+1}, \mathbf{h})_S + \frac{\alpha}{\epsilon} \\ &\times (\lambda_{k+1}\mathbf{n}, \mathbf{h})_S = (1-\alpha_k)\left[(|\nabla_s\mathbf{g}_k|^{r-2}\nabla_s\mathbf{g}_k, \nabla_s\mathbf{h})_S + (|\mathbf{g}_k|^{r-2}\mathbf{g}_k, \mathbf{h})_S\right] \\ &- \frac{\alpha_k}{\epsilon}(\mathbf{s}_{k+1}, \mathbf{h})_S, \quad \forall \mathbf{h} \in W^{1,r}(S).\end{aligned} \tag{4.28}$$

$$(\mathbf{g}_{k+1}, \mathbf{n})_S = 0. \tag{4.29}$$

The restriction $\int_S \mathbf{h}\cdot\mathbf{n}\, dS = 0$ on the control space M is taken care of by (4.29) in the variational formulation.

Remark 4.2. Note that the optimality condition yields a relation between the control and the adjoint stress force variable $\mathbf{s}$. The Dirichlet control is updated using $\mathbf{s}$ in (4.28), while Neumann control is determined by $\mathbf{w}$, the adjoint velocity variable in (3.13).

This is because the Dirichlet control affects the system through (4.18), not (4.17).

In the case that the $\nabla_s \mathbf{g}$ term is deleted from (4.22), the optimality condition is given as

$$\int_S \epsilon|\mathbf{g}|^{r-2}\mathbf{g}\cdot\mathbf{h} + \mathbf{s}\cdot\mathbf{h} + \lambda\mathbf{n}\cdot\mathbf{h}\, dS = 0. \tag{4.30}$$

Thus the control is updated by the explicit form

$$\mathbf{g}_{k+1} = \mathbf{g}_k - \frac{\alpha_k}{\epsilon}(\epsilon|\mathbf{g}_k|^{r-2}\mathbf{g}_k + \mathbf{s}_k + \lambda_k\mathbf{n}), \tag{4.31}$$

where, enforcing the condition (4.15)–(4.31), we can obtain the explicit formula for the lagrange multiplier λ_k:

$$\lambda_k = \frac{1}{|S|}\left(\frac{\epsilon}{\alpha}\int_S (1-\alpha|\mathbf{g}_k|^{r-2})\mathbf{g}_k\cdot\mathbf{n}\, dS - \int_S \mathbf{s}_k\cdot\mathbf{n}\, dS\right). \tag{4.32}$$

5. Mean pressure boundary condition

The optimization technique by boundary controls can be extended for other types of defective boundary condition, e.g., mean pressure boundary condition. Supposed we have mean pressure specified on defective boundaries:

$$\frac{1}{|S_i|}\int_{S_i} p dS = P_i \quad \text{for } i = 1,\ldots,m. \tag{5.33}$$

Since pressure is unique up to a constant, we may set $\mathbf{g}_1 = \mathbf{0}$, and p is shifted appropriately so that the mean pressure condition on S_1 is satisfied. Define the functional

$$\mathcal{J}(\mathbf{u},p,\boldsymbol{\sigma},\mathbf{g}) := \frac{1}{2}\sum_{i=1}^{m}\left(\frac{1}{|S_i|}\int_{S_i} p\, dS_i - P_i\right)^2 + \frac{\epsilon}{r'}\int_S |\mathbf{g}|^{r'} dS, \tag{5.34}$$

where $\mathbf{g}$ is the Neumann boundary control. Using the similar approach shown in previous sections, we can obtain the optimality system

$$v_0^{1-r'}(|\boldsymbol{\sigma}|^{r'-2}\boldsymbol{\sigma},\boldsymbol{\tau}) - (\mathbf{D}(\mathbf{u}),\boldsymbol{\tau}) = 0, \quad \forall\, \boldsymbol{\tau}\in\boldsymbol{\Sigma}, \tag{5.35}$$

$$(\boldsymbol{\sigma},\mathbf{D}(\mathbf{v})) - (p,\nabla\cdot\mathbf{v}) = (\mathbf{f},\mathbf{v}) + \frac{1}{\epsilon^{r/r'}}(|\mathbf{w}|^{r-2}\mathbf{w},\mathbf{v})_S, \quad \forall\, \mathbf{v}\in\mathbf{X}, \tag{5.36}$$

$$(q,\nabla\cdot\mathbf{u}) = 0, \quad \forall\, q\in P \tag{5.37}$$

and the adjoint equations

$$v_0^{1-r'}(r'-2)(|\boldsymbol{\sigma}|^{r'-4}(\boldsymbol{\sigma}:\boldsymbol{\eta})\boldsymbol{\sigma},\boldsymbol{\tau}) + v_0^{1-r'}(|\boldsymbol{\sigma}|^{r'-2}\boldsymbol{\eta},\boldsymbol{\tau}) + (\mathbf{D}(\mathbf{w}),\boldsymbol{\tau}) = 0, \quad \forall\, \boldsymbol{\tau}\in\boldsymbol{\Sigma}, \tag{5.38}$$

$$(\boldsymbol{\eta},\mathbf{D}(\mathbf{v})) + (\xi,\nabla\cdot\mathbf{v}) = 0, \quad \forall\, \mathbf{v}\in\mathbf{X}, \tag{5.39}$$

$$(q,\nabla\cdot\mathbf{w}) = \sum_{i=1}^{m}\left(\frac{1}{|S_i|}\int_{S_i} p\, dS_i - P_i\right)\int_{S_i} q\, dS_i, \quad \forall\, q\in P. \tag{5.40}$$

If Dirichlet control $\mathbf{g}$ is considered to minimize the penalized functional

$$\mathcal{J}(\mathbf{u},p,\boldsymbol{\sigma},\mathbf{g}) := \frac{1}{2}\sum_{i=1}^{m}\left(\frac{1}{|S_i|}\int_{S_i} p\, dS_i - P_i\right)^2 + \frac{\epsilon}{r}\int_S |\nabla_s\mathbf{g}|^r + |\mathbf{g}|^r\, dS \tag{5.41}$$

for the mean pressure matching, one needs to solve (4.16)–(4.18) and

$$v_0^{1-r'}(r'-2)(|\boldsymbol{\sigma}|^{r'-4}(\boldsymbol{\sigma}:\boldsymbol{\eta})\boldsymbol{\sigma},\boldsymbol{\tau}) + v_0^{1-r'}(|\boldsymbol{\sigma}|^{r'-2}\boldsymbol{\eta},\boldsymbol{\tau}) + (\mathbf{D}(\mathbf{w}),\boldsymbol{\tau}) = 0, \quad \forall\, \boldsymbol{\tau}\in\boldsymbol{\Sigma}, \tag{5.42}$$

$$(\boldsymbol{\eta},\mathbf{D}(\mathbf{v})) + (\xi,\nabla\cdot\mathbf{v}) + (\mathbf{s},\mathbf{v})_S = 0, \quad \forall\, \mathbf{v}\in\mathbf{X}, \tag{5.43}$$

$$(q,\nabla\cdot\mathbf{w}) + (\mathbf{z},\mathbf{w})_S = \sum_{i=1}^{m}\left(\frac{1}{|S_i|}\int_{S_i} pdS - P_i\right)\int_S qdS, \quad \forall\, (q,\mathbf{z})\in P\times(W^{1/r-1,r}(S))^n, \tag{5.44}$$

The same optimality condition (4.27) is obtained and the control $\mathbf{g}$ can be updated by (4.28) and (4.29).

6. Numerical results

In this section we present numerical results for a flow problem subject to specified flow rates conditions or mean pressure conditions on the defective boundaries. Along the other boundaries we impose the usual non-slip condition for the fluid velocity. We consider a model problem of flow in a square domain, $(0,5)\times(0,5)$, with boundaries where defective boundary conditions are imposed: $S_1 = \{(x,y): x=0, 1<y<2\}$, $S_2 = \{(x,y): x=0, 3<y<4\}$ on the left side of the domain and $S_3 = \{(x,y): x=5, 2<y<3\}$ on the right side. See Fig. 1. In the constitutive Eq. (1.1) the parameter r is chose as $r=\frac{3}{2}$ ($r'=3$). All computations were performed using 31×31 uniform grid. For the approximation of the velocity and pressure we used continuous piecewise quadratic and continuous piecewise linear finite elements, respectively, (i.e. the Taylor–Hood pair). For the approximation of the stress we used continuous piecewise linear finite elements. Note that the finite element spaces satisfy the inf–sup conditions (3.1), (3.2).

6.1. Flow rate boundary condition

For comparison purpose, first we computed velocity, pressure and stress using a standard Dirichlet boundary condition of parabolic profile on each S_i; $\mathbf{u} = \begin{bmatrix}-8(y-1)(y-2)\\0\end{bmatrix}$, $\begin{bmatrix}-4(y-3)(y-4)\\0\end{bmatrix}$, $\begin{bmatrix}-12(y-2)(y-3)\\0\end{bmatrix}$ on S_1, S_2, S_3, respectively. The magnitude of velocity and streamlines are given in Figs. 2, and 3 shows pressure profile and mean pressure on each defective boundary.

The Dirichlet boundary condition chosen yields flow rates $Q_1 = -4/3$, $Q_2 = -2/3$ and $Q_3 = 2$. These values were used as flow rate boundary conditions in the flow matching problem. For the optimization routine, the constant vector $\mathbf{g} = [0.1,\ldots,0.1]^T$ was used as an initial guess for both Dirichlet and Neumann controls. We selected the penalty parameter $\epsilon = 10^{-10}$ and the stopping criterion $\mathcal{J}(\mathbf{g}) < 10^{-6}$. Streamlines of fluid flow by the Neumann and Dirichlet controls are presented in Figs. 4 and 5, respectively. The horizontal velocity profiles on the defective boundaries are also shown in Figs. 6 and 7. The figures show the Neumann control yields velocity profile that looks more similar to the standard case

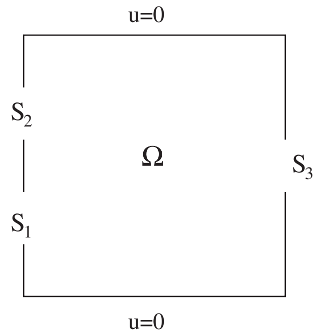

Fig. 1. The flow domain.

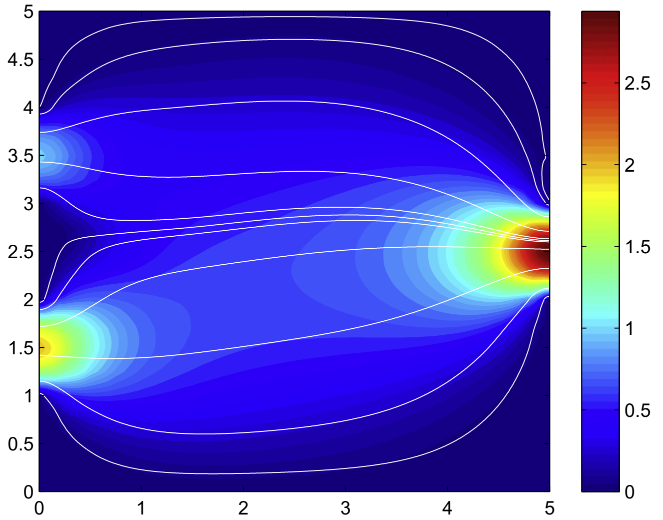

Fig. 2. Plot of the magnitude of the velocity and streamlines by the given Dirichlet boundary condition.

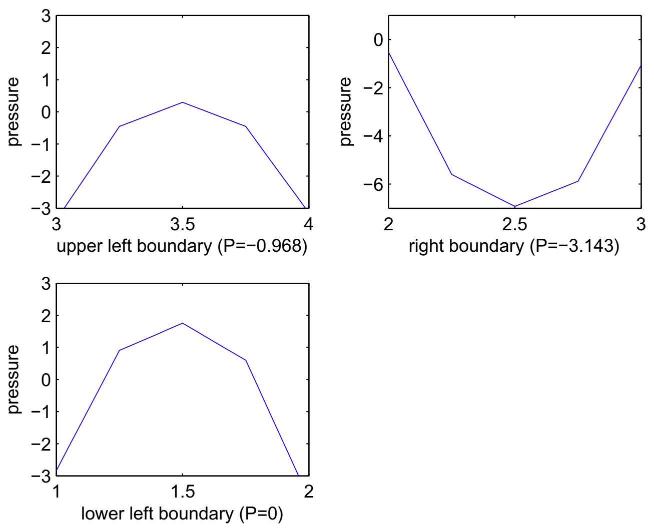

Fig. 3. pressure on boundaries S_0, S_1, S_2 by the given Dirichlet boundary condition.

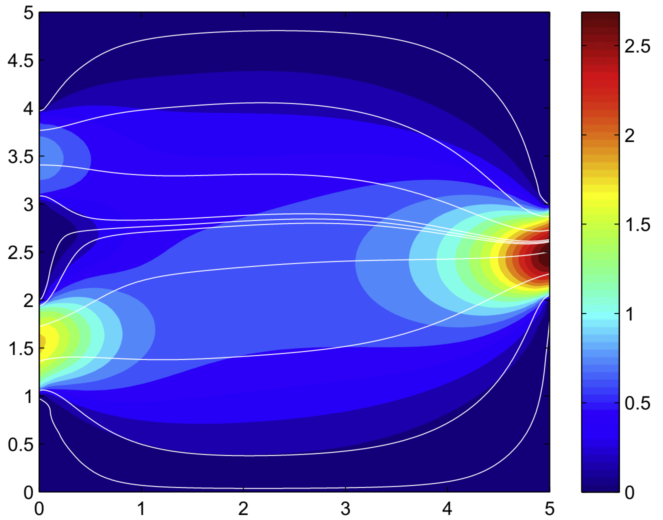

Fig. 4. Plot of the magnitude of the velocity and streamlines by Neumann boundary control.

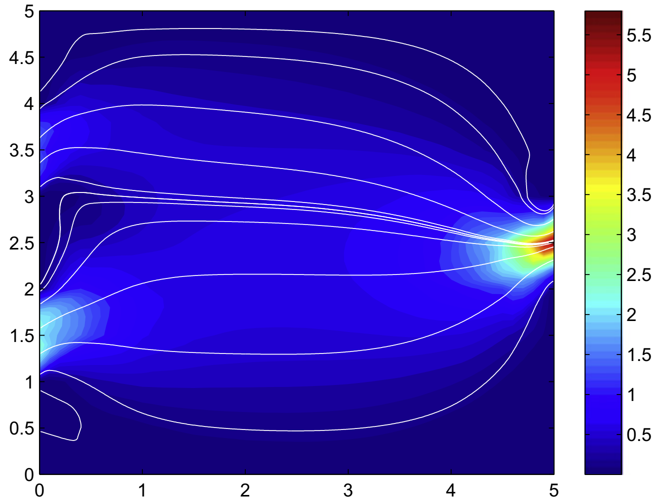

Fig. 5. Plot of the magnitude of the velocity and streamlines by Dirichlet boundary control.

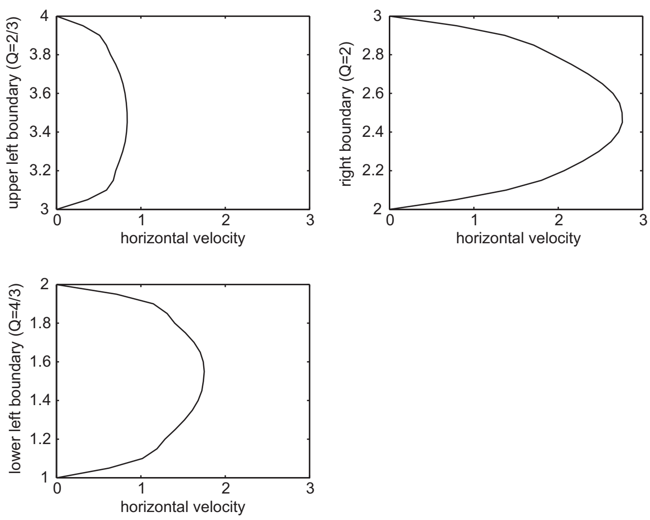

Fig. 6. Horizontal velocity profiles on boundaries S_0, S_1, S_2 by Neumann boundary control.

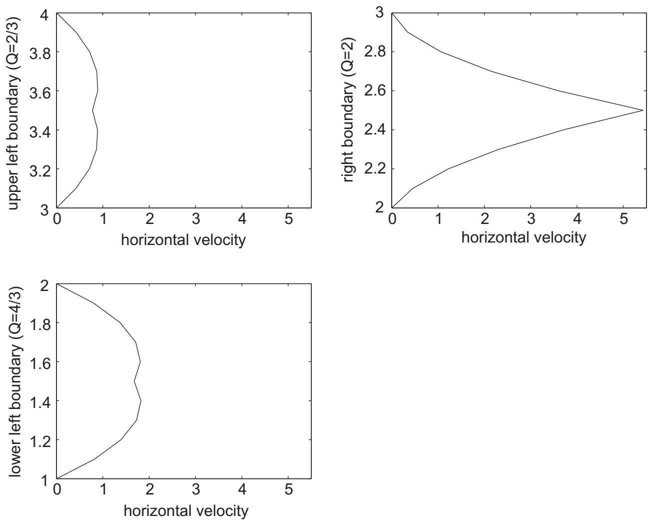

Fig. 7. Horizontal velocity profile on boundaries S_0, S_1, S_2 by Dirichlet boundary control.

of parabolic-shaped Dirichlet condition than the Dirichlet control. In fact, it was observed in numerical experiments that the Neumann control is more robust. The Dirichlet control is more sensitive to an initial guess, parameters chosen, and sometimes yields a non-physical solution with the objective functional still minimized within the tolerance. On the other hand, the Neumann control yielded consistent results in most simulations with different choices for an initial guess and parameters. As mentioned in the beginning of the paper, the defective boundary problem is not a well-posed problem. Also, when formulated as a control problem, an optimal solution is not unique for the model problem. The presented results should be understood as one possible solution satisfying the defective boundary conditions.

6.2. Mean pressure boundary condition

Using the Dirichlet boundary condition chosen we computed pressure and shifted the numerical solution so that P_1, the mean pressure on S_1, is 0. The pressure on S_2, S_3 were computed as $P_2 = -0.968$, $P_3 = -3.143$, and these values were used for the mean pressure matching problem. Streamlines of fluid flow by the

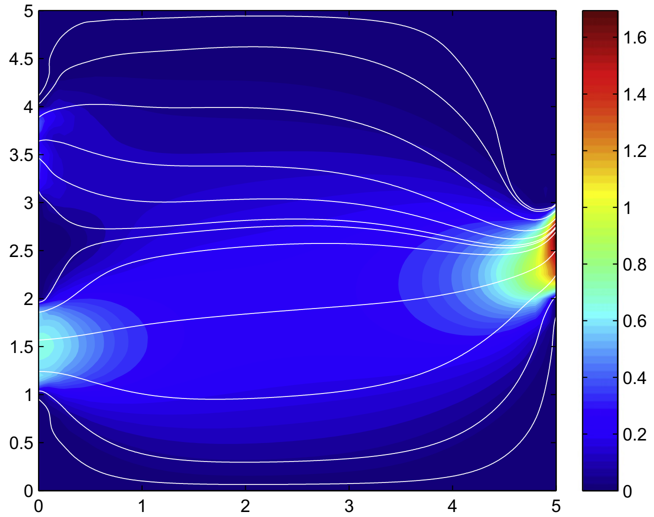

Fig. 8. Plot of the magnitude of the velocity and streamlines by Neumann boundary control.

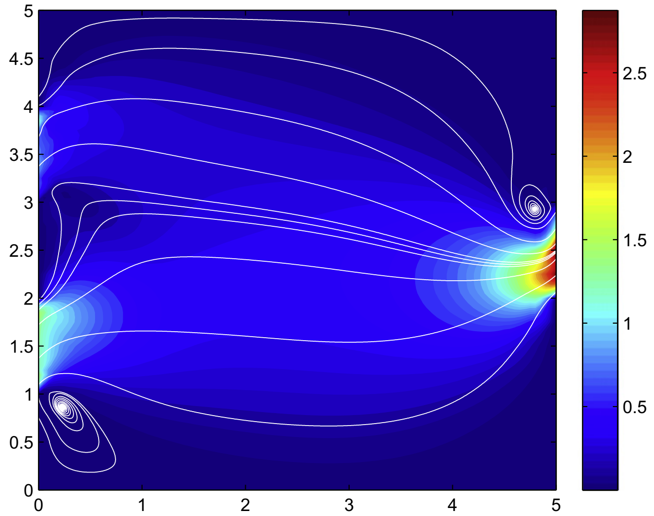

Fig. 9. Plot of the magnitude of the velocity and streamlines by Dirichlet boundary control.

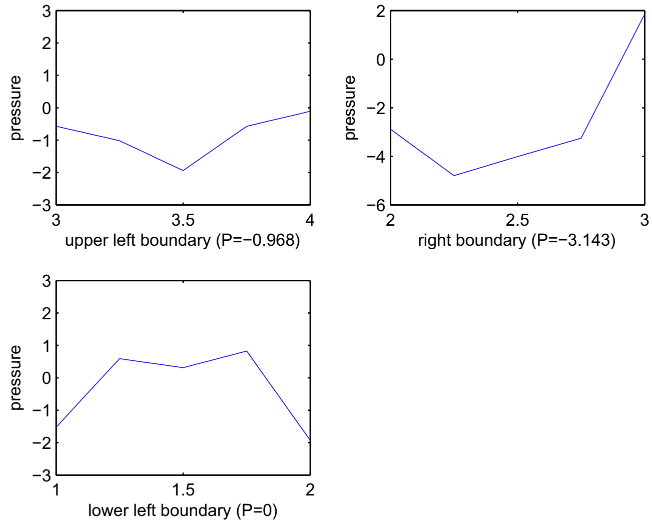

Fig. 10. Pressure on boundaries S_0, S_1, S_2 by Neumann boundary control.

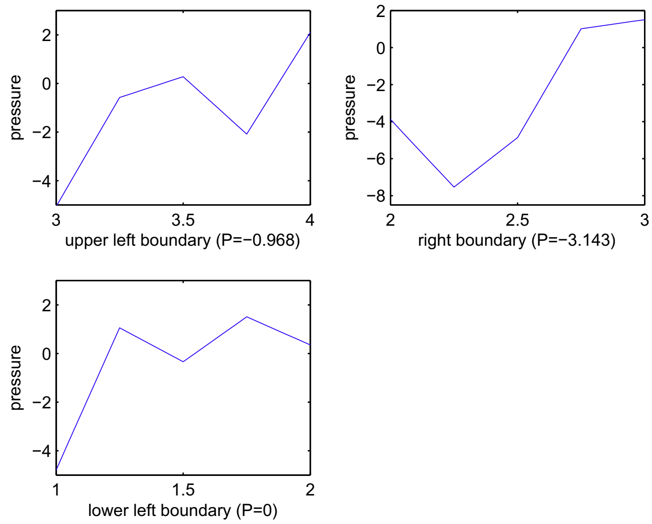

Fig. 11. Pressure on boundaries S_0, S_1, S_2 by Dirichlet boundary control.

Neumann and Dirichlet controls are presented in Figs. 8 and 9, respectively. The pressure profiles on the defective boundaries are also shown in Figs. 10 and 11. As in the flow matching problem, the Neumann control yielded similar results to the standard case shown in Fig. 2, and was more robust than the Dirichlet control.

7. Concluding remarks and future work

We studied defective boundary condition problems using the optimal control technique by introducing Neumann or Dirichlet type control. The similar approach may be considered for time-dependent unsteady flows or more complex fluids. As an extension of this work, we will consider non-Newtonian, viscoelastic fluid flows governing by the *Oldroyd-B* model

$$\boldsymbol{\sigma} + \lambda\left(\mathbf{u}\cdot\nabla\boldsymbol{\sigma} + (\nabla\mathbf{u})^T\boldsymbol{\sigma} - \boldsymbol{\sigma}\nabla\mathbf{u}\right) - 2\alpha D(\mathbf{u}) = \mathbf{0} \quad \text{in } \Omega, \tag{7.45}$$

$$-\nabla\cdot\boldsymbol{\sigma} - 2(1-\alpha)\nabla\cdot D(\mathbf{u}) + \nabla p = \mathbf{f} \quad \text{in } \Omega, \tag{7.46}$$

$$div\ \mathbf{u} = 0 \quad \text{in } \Omega, \tag{7.47}$$

where λ is the Weissenberg number defined as the product of the relaxation time and a characteristic strain rate, and α is a number such that $0 < \alpha < 1$ which may be considered as the fraction of viscoelastic viscosity.

Unlike in the quasi-Newtonian fluid, the extra stress of viscoelastic fluids is coupled with the velocity through a nonlinear constitutive equation. Since the viscoelastic fluid is a fluid with memory, some information on flow history should be provided when entering into a fluid domain, thus, a stress boundary condition needs to be specified on inflow boundaries in order to be a well-posed problem. We will assume no boundary information on the velocity and the stress provided except the flow rates condition (1.5). This defective boundary condition problem can be formulated as a two-parameter control problem by introducing a Neumann control for velocity on S and Dirichlet control for stress on S_{in}, the inflow defective boundary. Results of this problem will be reported in the later paper.

Acknowledgement

Partially supported by the NSF under Grant No. DMS-1016182.

References

[1] F. Abrahan, M. Behr, M. Heinkenschloss, Shape optimization in unsteady blood flow: A numerical study of non-Newtonian effects, Comput. Methods Biomech. Biomed. Engrg. 8 (2005) 201–212.
[2] J. Baranger, K. Najib, D. Sandri, Numerical analysis of a three-fields model for a quasi-Newtonian flow, Comput. Methods Appl. Mech. Engrg. 109 (1993) 281–292.
[3] J. Burkardt, M. Gunzburger, Sensitivity discrepancy for geometric parameters, CFD Design Optim. (1995) 5–15.
[4] P. Ciarlet, The Finite Element Method for Elliptic Problems, North-Holland, Amsterdam, 1978.
[5] Q. Du, M. Gunzburger, L.S. Hou, Analysis and finite element approximation of optimal control problems for a Ladyzhenskaya model for stationary, incompressible viscous flows, J. Comput. Appl. Math. 61 (1995) 323–343.
[6] V.J. Ervin, T.N. Phillips, Residual a posteriori error estimator for a three-field model of a non-linear generalized Stokes problem, Comput. Methods Appl. Mech. Engrg. 195 (2006) 2599–2610.
[7] V.J. Ervin, H. Lee, Numerical approximation of a quasi-Newtonian Stokes flow problem with defective boundary conditions, SIAM J. Numer. Anal. 45 (2007) 2120–2140.
[8] L. Formaggia, J.F. Gerbeau, F. Nobile, A. Quarteroni, Numerical treatment of defective boundary conditions for the Navier–Stokes equations, SIAM J. Numer. Anal. 40 (2002) 376–401.
[9] L. Formaggia, A. Veneziani, C. Vergara, A new approach to numerical solution of defective boundary value problems in incompressible fluid dynamics, SIAM J. Numer. Anal. 46 (2008) 2769–2794.
[10] G.N. Gatica, M. Gonzlez, S. Meddahi, A low-order mixed finite element method for a class of quasi-Newtonian Stokes flows. I.A priori error analysis, Comput. Methods Appl. Mech. Engrg. 193 (2004) 881–892.
[11] M.D. Gunzberger, Perspectives an Flow Control and Optimization, SIAM, 2003.
[12] M. Gunzburger, L. Hou, T. Svobodny, Heating and cooling control of temperature distributions along boundaries of flow domains, J. Math. Syst. Estimat. Control 3 (1993) 147–172.
[13] Max Gunzburger, H.-C. Lee, Analysis, approximation, and computation of a coupled solid/fluid temperature control problem, Comput. Methods Appl. Mech. Engrg. 118 (1–2) (1994) 133–152.
[14] M. Gunzburger, H. Wood, Adjoint and sensitivity-based methods for optimization of gas centrifuges, in: Proceedings of 7th Work. Separation Phenomena in Liquids and Gases; Moscow Engineering Physics Institute, 2000, pp. 89–99.
[15] J.G. Heywood, R. Rannacher, S. Turek, Artificial boundaries and flux and pressure conditions for the incompressible Navier–Stokes equations, Int. J. Numer. Methods Fluids 22 (1996) 325–352.
[16] H. Lee, H.C. Lee, Analysis and finite element approximation of an optimal control problem for the Oseen viscoelastic fluid flow, J. Math. Anal. Appl. 336 (2007) 1090–1160.
[17] H. Manouzi, M. Farhloul, Mixed finite element analysis of a non-linear three-fields Stokes model, IMA J. Numer. Anal. 21 (2001) 143–164.
[18] D. Sandri, A posteriori estimators for mixed finite element approximations of a fluid obeying the power law, Comput. Methods Appl. Mech. Engrg. 166 (1998) 329–340.
[19] A. Veneziani, C. Vergara, Flow rate defective boundary conditions in haemodynamics simulations, Int. J. Numer. Methods Fluids 47 (2005) 803–816.
[20] E. Zeidler, Nonlinear Functional Analysis and its Applications II/B: Nonlinear Monotone Operators, Springer-Verlag, 1990.